3D Homogeneous Turbulence

April 14, 2021

In this chapter we focus on what can be called the purest turbulence problem, as well as the classical one. It is in fact so pure that, strictly speaking, it cannot exist in nature, although experience shows that natural turbulence often has behavior remarkably close to the pure form. This is the case where rotational and gravitational forces are negligible (*i.e.,* $g = f = 0$); b or c can be considered to represent a generic passive tracer (or neglected altogether); all boundary influences are ignored; there is no mean shear at least not on the (small) scales of interest; and the statistics are spatially isotropic and homogeneous and temporally either stationary (in equilibrium) or simply decaying from a specified initial condition. In a strict sense, therefore, the domain must be infinite in extent and the time span infinite in duration, but it is often assumed to be spatially periodic on a scale large compared to the motions of interest, and the integration or sampling interval must be large enough (*e.g.,* compared to an eddy turnover time) to achieve satisfactory statistical accuracy. With periodic boundary conditions the rotation symmetry (*i.e.,* equivalence with respect to a coordinate rotation about any axis; this is the same as the isotropy symmetry discussed below) is only approximately valid, but presumably more so on the smaller scales than the larger, domain-influenced ones. But a periodic domain is more readily computable than an infinite one, and in laboratory experiments the domains are both finite and have non-periodic boundaries.

The essential governing equations are

$$\begin{aligned} \frac{D\mathbf{u}}{Dt} &= -\nabla\phi + \nu\nabla^2\mathbf{u} \\ \nabla\cdot\mathbf{u} &= 0 \end{aligned} \tag{1}$$

with any passive tracer equation having an advection-diffusion balance, *viz.,*

$$\frac{Dc}{Dt} = \kappa\nabla^2 c\,.$$

These equations are equally valid in 3D or 2D, although their dynamical behaviors are quite different for homogeneous turbulence; so we shall discuss them separately[1]. There is a famous Millennium Prize offered by the Clay Mathematical Institute for the solution of any of seven classical mathematical problems, one of which is the proof of existence and long-time smoothness, or not, of solutions of (1) with smooth initial and boundary conditions in 3D. This proof has already been made in 2D (Ladyzhenskaya, 1969), and the crucial distinction with 3D is the Lagrangian conservation of vorticity in 2D (*i.e.,* the lack of vorticity amplification through stretching).

3D homogeneous turbulence is relevant to geophysical turbulence on small scales away from boundaries. In the presence of rotation, stable stratification, and mean velocity shear, the necessary

[1]There is an analogous equation in 1D, called *Burgers Equation*, that does embody advection and diffusion:

$$\frac{\partial v}{\partial t} + v\frac{\partial v}{\partial x} = \nu\frac{\partial^2 v}{\partial x^2}\,.$$

However, lacking incompressibility, pressure-gradient force, and vorticity, its solution behavior (sometimes called *burgulence*) is rather different than in 2D and 3D fluid dynamics. At large Re values, it develops near discontinuities in space in finite time, and thus it is more like steepening nonlinear waves (*e.g.,* shocks) than like vortical turbulence.

conditions for this to be true are that Rossby, Froude, and shear numbers,

$$Ro \;=\; \frac{V}{fL}\,, \quad Fr \;=\; \frac{V}{NH}\,, \quad \& \quad Sh \;=\; \frac{V}{SL}\,,$$

are very large. Here f is the Coriolis frequency, $N = \sqrt{d\overline{b}/dz}$ is the mean stratification frequency; H is a vertical length scale (*i.e.,* in the direction of the stratification); and $S = d\overline{U}/dy$ is the mean shear. These numbers can be large either because the environmental frequencies ($f,\ N,\ S$) are small or because the turbulent velocity is large and/or the turbulent length scale is small.

The approach we take here is a phenomenological one, based more on intuitive concepts and rough estimates than on precise definitions, theories, and elaborate models. Of course, there is a large literature on the latter topics, but they are not our focus. There is some repetition of the material in *Turbulent Flows: General Properties* but with greater elaboration here.

1 Symmetries

The mathematical symmetries of the PDE system (1) with $f \;=\; g \;=\; 0$ include the following[2] (forcing, boundary, and initial conditions permitting):

- *homogeneity:* $\mathbf{x}$ translation, $\mathbf{x} \leftrightarrow \mathbf{x} + \mathbf{x}_0$ (*i.e.,* a uniform displacement or origin shift);
- *stationarity:* t translation, $t \leftrightarrow t + t_0$;
- *Galilean invariance:* $\mathbf{u}$ translation, $\mathbf{u} \leftrightarrow \mathbf{u} + \mathbf{u}_0$;
- *isotropy:* $\mathbf{x}$ rotation, $\mathbf{x} \leftrightarrow \mathbf{x}\, e^{i\theta_0}$ (in complex notation);
- *reflection or parity reversal:* $(\mathbf{u}, \mathbf{x}, t) \leftrightarrow (-\mathbf{u}, -\mathbf{x}, t)$;
- *time reversibility:* (for $\nu = 0$): $(\mathbf{u}, \mathbf{x}, t) \leftrightarrow (-\mathbf{u}, \mathbf{x}, -t)$;
- *scaling:* (for $\nu \;=\; 0$) $(\mathbf{u}, \mathbf{x}, t) \;\leftrightarrow\; (\lambda^h \mathbf{u}, \lambda \mathbf{x}, \lambda^{1-h} t) \;\; \forall\ \lambda,\ h$ [this says there is no intrinsic velocity, space, or time scale to turbulence — it's all relative!];
- the so-called *similarity principle of fluid dynamics* (really just non-dimensionalization with $\nu \;\neq\; 0$): as a viscous extension of the scaling symmetry, either $\nu \;\leftrightarrow\; \lambda^{1+h} \nu \;\; \forall\ \lambda,\ h$ **or** $\nu \leftrightarrow \nu \;\; \forall \lambda$ and $h = -1$, which leaves Re unchanged;

$$Re \;=\; \frac{VL}{\nu} \;\leftrightarrow\; \left\{ \lambda^h \times \frac{\lambda}{\lambda^{1+h}} \textbf{ or } \lambda^0) \right\} \cdot \frac{VL}{\nu}\,.$$

Symmetries, both here and as generally in theoretical physics, strongly constrain the possible physical outcomes and their interpretation.

One view of intermittency is that it occurs by having scale invariance (*i.e.,* independence of λ) for different values of the scaling exponent h in different $(\mathbf{x}, t)$ regions within the same flow realization. This is called a *multi-fractal* view. In this view turbulent flows have one kind of space-time structure locally and different kinds in other places and times.

[2]There are analogous symmetries for the passive scalar equation, but they are not explicitly listed here. The same symmetries apply equally in 3D and 2D.

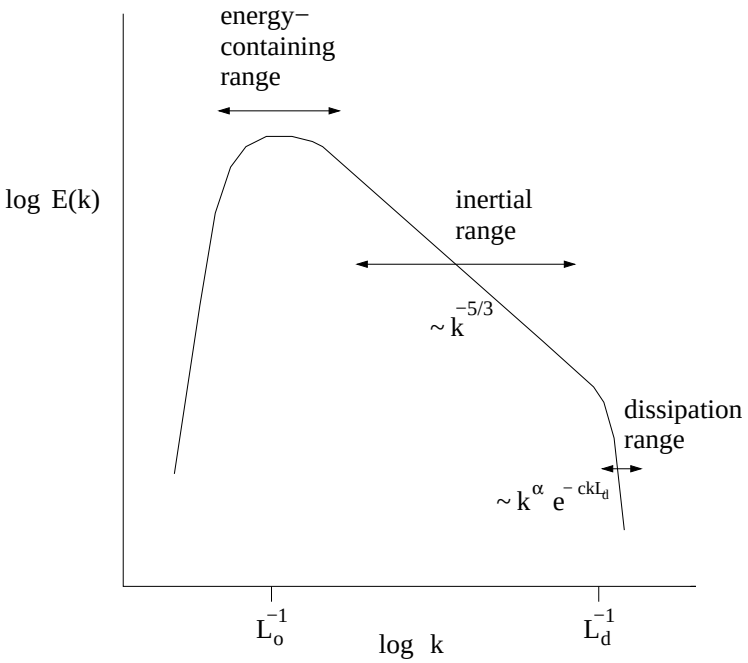

Figure 1: A cartoon of the isotropic kinetic energy spectrum in equilibrium 3D homogeneous turbulence, presuming a forcing near the outer scale L_o. Symbols are defined in the text.

2 Kolmogorov's Phenomenological Theory

[Sometimes this is called K41 theory, after Kolmogorov (1941).] Consider a minimal description of turbulence where we assume that it is characterized only by the following quantities: the kinetic energy E; an "outer" spatial scale (*i.e.,* the largest or most energetic one for which the homogeneous assumption is valid) L_o; any smaller scale L; the viscosity ν; and the energy dissipation rate ε. The outer velocity scale is implicit here, $V_o = \sqrt{2E}$, as is the outer-scale Reynolds number, $Re_o = V_o L_o/\nu$. These scales are the ingredients for dimensional reasoning. We consider a Fourier transform of $\mathbf{u}$ that allows a decomposition of the total energy in wavenumber magnitude k,

$$E \;=\; \int dk\, E(k)\;, \tag{2}$$

where we make the association $k \sim 1/L$. Using the isotropy assumption, we only need to consider one scalar wavenumber magnitude, $k = |\mathbf{k}|$, and its associated energy density $E(k)$ related to the total energy spectrum by

$$\int_0^\infty dk\, E(k) \;=\; \frac{1}{2} \int d\mathbf{k}\, |\hat{\mathbf{u}}|^2(\mathbf{k})\;. \tag{3}$$

We are interested in the overall evolution and transformation rates of the system, expressed in terms of the kinetic energy spectrum:

Cascade: $\delta E(k)/\delta t$ such that $[E(k_1),\, E(k_2)] \;\longrightarrow\; [E(k_1){-}\delta E,\, E(k_2){+}\delta E]$. For 3D turbulence this occurs for $k_1 < k_2$, but for 2D turbulence the transfer is primarily from k_2 to k_1 (see 2D Homogeneous Turbulence notes).

Dissipation: $\delta E/\delta t \;=\; -\varepsilon$.

Transport: $\overline{c'\mathbf{u}'}$ for any fluid property c, where we can expect differences depending upon whether c is momentum or a passive scalar (*n.b.,* $\overline{c'\mathbf{u}'} = 0$ whenever $\nabla\overline{c} = 0$, as in a wholly homogeneous situation).

Now consider three hypotheses about the nature of the cascade and dissipation processes. These were proposed by Frisch (1995) as a formalization of the seminal theory of Kolmogorov (1941), which we will follow here. It is a phenomenological theory based on a physical conception of turbulent behavior. It also is a scaling theory declaring how flow properties vary with the spatial scale L.

H1: As $Re \to \infty$, all the possible symmetries discussed in Sec. 1 (except for the arbitrariness of the exponent h in the scaling symmetry) — which may broken by the mechanisms producing the turbulence (*i.e.,* the dynamics involving f, g, $\nabla\overline{\mathbf{u}}$, and $\nabla\overline{b}$) — are restored in a statistical sense at small scales and away from boundaries.

H2: Under these conditions the turbulence is self-similar at small scales; *i.e.,* it possesses a unique scaling exponent h,

$$\delta\mathbf{u}(\lambda L) \;=\; \lambda^h \delta\mathbf{u}(L), \tag{4}$$

for velocity differences $\delta\mathbf{u}$ over a spatial increment L, where both L and λL are in the small-scale range, $< L_o$.

H3: Under these conditions there exists a unique, finite value of ε.

The first hypothesis is one of *universality*, *viz.,* all physical regimes of turbulence are alike at small scales and large Re. The second hypothesis is a collapse of the general scaling symmetry by the selection of a dominant exponent h (*i.e.,* not multi-fractal behavior). The third hypothesis is the one that sets the value of h by declaring that the dissipation rate, equated with the cascade rate, is the physically most important quantity in turbulence.

An advective evolution is one where an eddy turn-over time τ is the relevant time for a significant change in the flow to occur due to differences in relative motion V_L acting through the advection operator:

$$\tau_L \;=\; \frac{L}{V_L} \tag{5}$$

on spatial scale L. The outer time scale,

$$\tau_o \;=\; \frac{L_o}{V_o}\,, \tag{6}$$

is the characteristic evolution time for the turbulent system dynamics as a whole.

We can determine a dissipation velocity and length, V_d and L_d, from the definition of ε,

$$\varepsilon \;=\; \nu\, \nabla\mathbf{u} : \nabla\mathbf{u}\,,$$

and a scaling estimate is

$$\varepsilon \sim \nu \frac{V_d^2}{L_d^2} . \tag{7}$$

If we assume that ν and ε are the only relevant quantities for the dissipation process (H3), then the other associated quantities are uniquely determined to be

$$\begin{aligned} V_d &\sim (\nu\varepsilon)^{1/4} = (\varepsilon\eta)^{1/3} \\ L_d &\sim \left(\frac{\nu^3}{\varepsilon}\right)^{1/4} \\ \tau_d &\sim \left(\frac{\nu}{\varepsilon}\right)^{1/2} . \end{aligned} \tag{8}$$

These are called the dissipation scales, and $L_d = \eta$ in particular is called the *Kolmogorov length scale*. Note that

$$\tau_d \sim \frac{L_d^2}{\nu} , \tag{9}$$

i.e., the diffusive and advective time scales are equal at L_d; hence, the diffusive rate is dominant at all scales smaller than L_d, which is thus referred to as the *dissipation range*.

The energy flux in the cascade at scale $L > L_d$ has

$$\frac{\delta E_L}{\delta t} \sim \frac{V_L^2}{\tau_L} \sim \frac{V_L^3}{L} , \tag{10}$$

where E_L is the energy at L (to be identified with the energy density $E(k)$ in (2) multiplied by a wavenumber increment, Δk). There is an assumption of independence from L of the energy flux extending from $L \to L_o^-$ to $L \to L_d^+$, hence its equality with ε, implies

$$\frac{V_L^3}{L} \sim \varepsilon, \tag{11}$$

at all L, or

$$V_L \sim (\varepsilon L)^{1/3} \quad \& \quad \tau_L \sim \varepsilon^{-1/3} L^{2/3}. \tag{12}$$

The hypothesis of self-similarity in the cascade range (H2) implies

$$\begin{aligned} V_{\lambda L} &\sim \lambda^h V_L \\ \varepsilon^{1/3}(\lambda L)^{1/3} &\sim \lambda^h (\varepsilon L)^{1/3} \\ &\Rightarrow h = \frac{1}{3} . \end{aligned} \tag{13}$$

The spatial-lag velocity covariance function is defined by

$$C_u(\mathbf{r}) = \overline{u(\mathbf{x})u(\mathbf{x}+\mathbf{r})} , \tag{14}$$

and the associated structure function is

$$S_u(\mathbf{r}) = \overline{(\, u(\mathbf{x}) - u(\mathbf{x}+\mathbf{r})\,)^2} \sim V_L^2 , \tag{15}$$

for $\mathbf{r} \sim L$. For a statistically homogeneous, isotropic situation, the two are related by

$$S_u(\mathbf{r}) = 2(\,\overline{u^2} - C_u(\mathbf{r})\,)\,. \tag{16}$$

The energy spectrum is the Fourier transform of C_u, and it expressed as

$$\begin{aligned} E(k) &\sim V_L^2 L \\ &\sim (\,(\varepsilon L)^{1/3})^2 L = \varepsilon^{2/3} L^{5/3} \\ &= C_k \varepsilon^{2/3} k^{-5/3}\,, \end{aligned} \tag{17}$$

where C_k is the Kolmogorov constant and has a value of about 1.6 in many experimental data. This is the famous Kolmogorov universal spectrum of turbulence (H1). One could, of course, immediately obtain the result (17) as the only dimensionally consistent combination of ε and L (*i.e.,* by an assumption that these are the only relevant quantities for the cascade). The range of scales, $L_o > L > L_d$, for which (12)-(17) holds, is referred to as the *inertial cascade range*.

The complete spectrum of 3D turbulence for all L can be depicted as shown in Fig. 1. The spectrum peak occurs at large scales in the *energy-containing range*, where it is well known that the particular shape of $E(k)$ depends on the particular physical regime and the mechanism of turbulence generation. At intermediate scales (*i.e.,* in the inertial range) the spectrum shape is (17) and is assumed to be universal (H1). At scales smaller than the dissipation scale L_d (*i.e.,* in the dissipation range), the spectrum falls off due to the disappearance of kinetic energy into the thermal reservoir of molecular collisions (*i.e.,* "heat death"), and its shape is steeper than any power law, often taken to have a shape

$$E(k) \;\propto k^{\alpha} e^{-ck/k_d}$$

as $k \to \infty$, where numerical calculations indicate that $\alpha \approx 3.3$ and $c \approx 7.1$ (Chen *et al.*, 1993). The dissipation range spectrum is also universal if the inertial range is. Note that the total energy E is not universal; it depends on the particular dynamics of the energy-containing range and also depends weakly on the scale separation between L_o and L_d when Re is finite.

There is considerable experimental and observational evidence in support of the Kolmogorov spectrum shape (17), *e.g.,* Fig. 2 from various experiments. There is also good experimental support for an approximately universal shape for the dissipation range (Fig. 3).

Another important length scale in turbulence is the *Taylor microscale* λ, defined as the square root of the ratio of the variances of the velocity and the velocity gradient. We can estimate the former as $\sim V_o^2$ and the latter as $\sim \varepsilon/\nu$ from the definition of dissipation in the energy budget; hence,

$$\lambda \;=\; \left[\frac{V_0^2}{\varepsilon}\nu\right]^{1/2} \;=\; \left[\frac{\nu L_o}{V_o}\right]^{1/2}\,, \tag{18}$$

where the continuity of cascade, $\varepsilon \;\sim\; V_o^3/L_o$, is used to obtain the last relation. This scale is intermediate between L_o and L_d since we can derive the ratios

$$\frac{\lambda}{L_d} \;=\; Re^{1/4} \;\;\text{and}\;\; \frac{L_o}{\lambda} \;=\; Re^{1/2}\,. \tag{19}$$

The last of these implies that an alternative Reynolds number based on λ,

$$Re_\lambda \;=\; \frac{V_o \lambda}{\nu}\,, \tag{20}$$

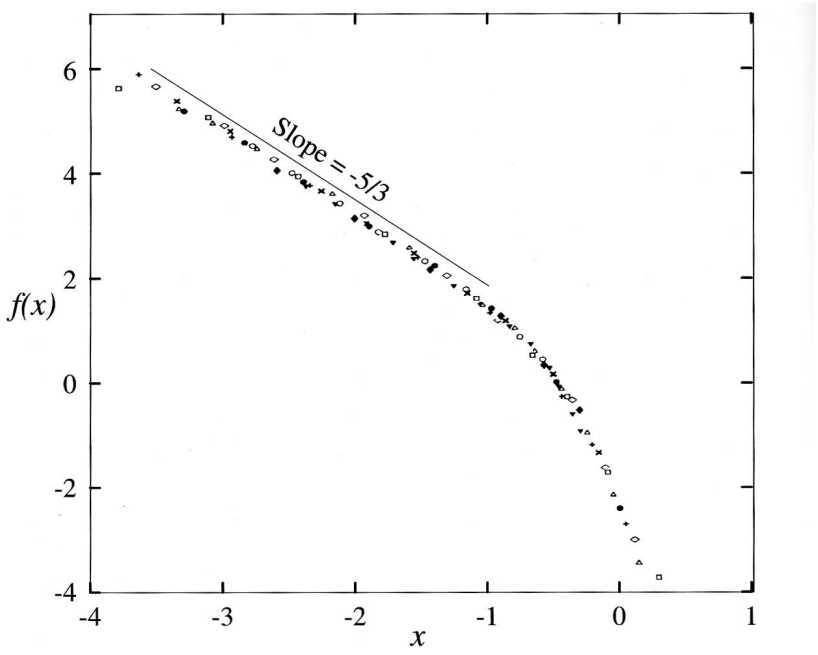

Figure 2: Normalized energy spectra from nine different turbulent flows with Re_λ values ranging from 130 to 13,000, plotted in log-log coordinates. The wavenumber and energy spectrum have been divided by $\ln[Re_\lambda/Re_*]$ with $Re_* = 75$, and the resulting curves have been shifted to give the best possible superposition. (Gagne and Castaing, 1991; also see Grant *et al.*, 1961)

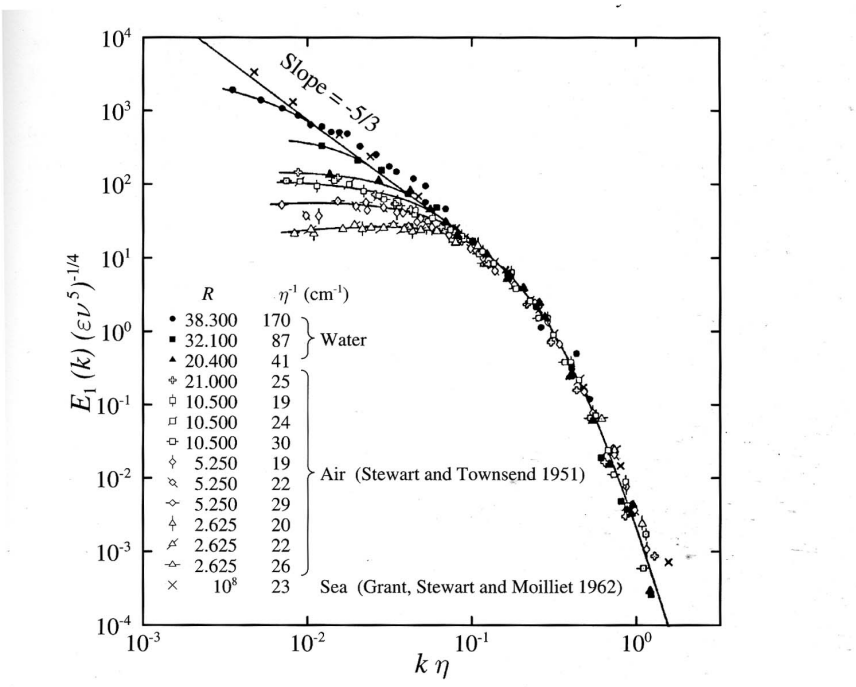

Figure 3: Normalized longitudinal velocity spectra according to different authors. The normalization is by dissipation scale quantities. (Gibson and Schwarz, 1963)

satisfies the relation $Re_\lambda = Re^{1/2}$. Re_λ is often used for observational estimates of the Reynolds number since both velocity and velocity derivative estimates are easily determined from a single time series (*e.g.,* Fig. 5). Finally, we can estimate the scale-local Reynolds number in the inertial range by

$$Re_L = \frac{V_L L}{\nu} = \left(\frac{L}{\eta}\right)^{4/3}, \tag{21}$$

which decreases as L decreases toward η; note that $Re_\eta = Re_d = 1$, as expected from an advection = diffusion balance at the Kolmogorov scale.

3 Cascade Dynamics

A visualization of the velocity and vorticity fields is in Fig. 4. Because the energy spectrum is not very steep, they emphasize the larger and smaller scale components of the flow, respectively.

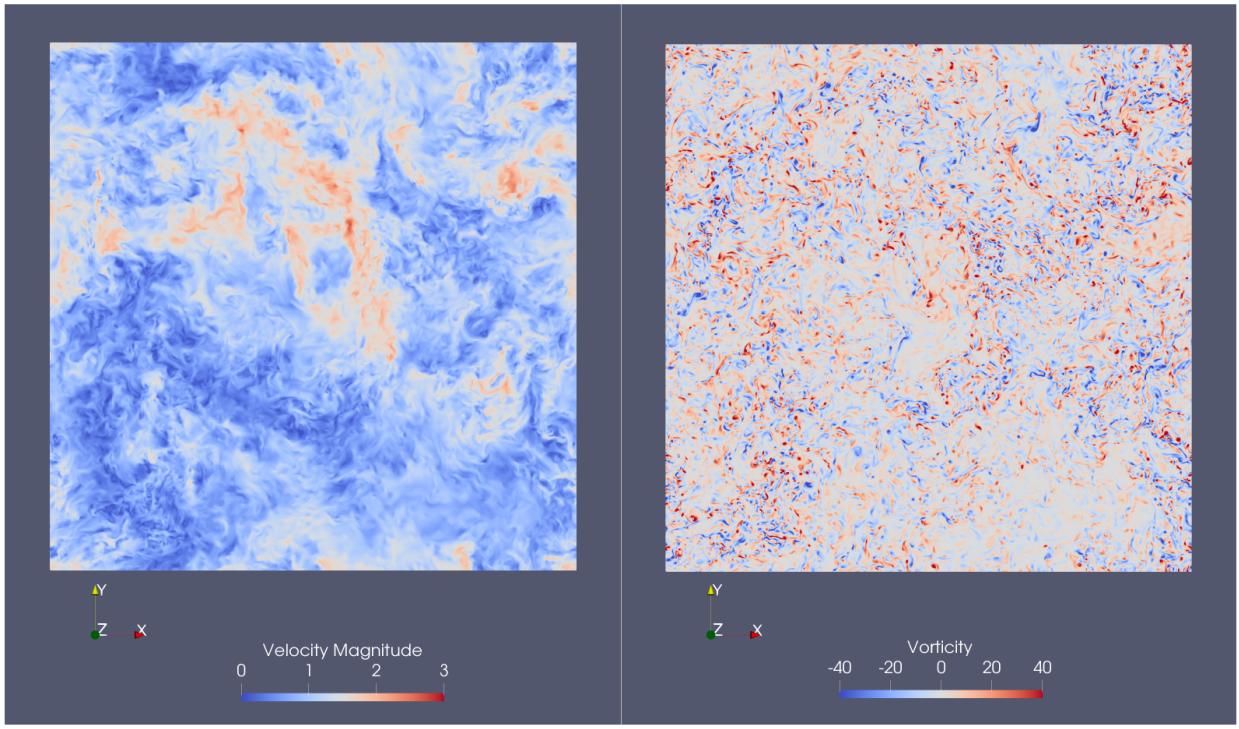

Figure 4: A cross-section through a simulation of equilibrium 3D turbulence at large Re: (left) velocity and (right) vorticity magnitudes. The vorticity "dots" can be interpreted as intersections thought the coherent vortex tubes in Figs. 14 and 16. (Johnson, 2020)

A central question in the theory of 3D homogeneous turbulence is how is energy transferred from large scales to small. The question is slightly ill-posed because the energy in a wavenumber spectrum $E(\mathbf{k})$ is non-locally related to the flow field $\mathbf{u}(\mathbf{x})$, just by the nature of a Fourier transform. Nevertheless, this question is often posed in terms of two different local flow configurations:

vortex stretching and strain-self amplification (Fig. 5). The vorticity field itself (Fig. 4, right) suggests the importance of the former, as has been the longer view historically, but recent analyses of simulations additionally gives support for the latter.

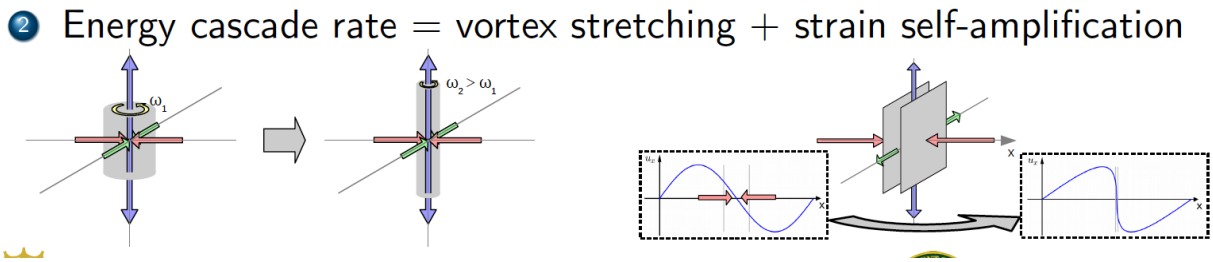

Figure 5: Sketches of the dynamical mechanisms for forward energy cascade in 3D homogeneous turbulence: (left) vortex stretching and (right) strain self-amplification. (Johnson, 2020)

In the Turbulent Flows lecture, the vorticity and strain rate were defined using index notation with a summation convention:

$$\zeta_i \;=\; \epsilon_{ijk}\partial_j u_k\,, \qquad S_{ij} \;=\; \frac{1}{2}(\partial_i u_j + \partial_j u_i)\,. \tag{22}$$

For both of these a relevant quantity is the velocity gradient tensor, $A_{ij} \;=\; \partial_i u_j$, where $\zeta_i \;=\; \epsilon_{ijk}(A_{kj} - A_{jk})/2$ and $S_{ij} \;=\; (A_{ij} + A_{ji})/2$, *i.e.,* the anti-symmetric and symmetric parts of A_{ij}. The squared magnitude of A_{ij} is called the Frobenius norm,

$$\mathcal{F} \;=\; \frac{1}{2}A_{ij}A_{ij} \;=\; \frac{1}{4}\zeta_i\zeta_i \;+\; \frac{1}{2}S_{ij}S_{ij}\,, \tag{23}$$

with separate contributions from vorticity and strain rate. One can show that on average the two components of $\mathcal{F}$ are equal, so that $|S|^2$ is smaller than $|\zeta|^2$. A local evolution equation for $\mathcal{F}$ is

$$\begin{aligned} \frac{D}{Dt}\mathcal{F} \;&=\; \mathcal{P}_\zeta + \mathcal{P}_s + O(\nu)\,. \\ \mathcal{P}_\zeta \;&=\; \frac{1}{4}\,\zeta_i S_{ij}\zeta_j \\ \mathcal{P}_S \;&=\; -\,S_{ij}S_{jk}S_{ki}\,, \end{aligned} \tag{24}$$

again with separate production contributions mainly associated with vorticity and entirely associated with strain. In this discussion we are not considering the viscous dissipation term $O(\nu)$.

In Fourier space, after averaging over wavenumber direction, the energy balance equation is

$$\partial_t E(k) \;=\; -\,\partial_k \Pi(k) + O(\nu)\,. \tag{25}$$

$\Pi(k) \;>\; 0$ represents the forward energy transfer rate across wavenumber k. In an equilibrium inertial range, $\partial_t E \;=\; 0$, and Π is independent of k (*i.e.,* Kolmogorov's constant cascade rate, equal to the dissipation rate ε). One can further show that in this range $\Pi \;\approx\; \Pi_\zeta + \Pi_S$ plus some smaller non-local (in k) transfer terms, and that $\Pi_S \;\approx\; 3\Pi_\zeta \;>\; 0$. Furthermore, in a spectral sense, $\Pi(k) \;=\; |\widehat{\mathcal{P}}|/k^2$ for both the ζ and S components, where $\widehat{\mathcal{P}}(k)$ is the wavenumber-space

representation of $\mathcal{P}(\mathbf{x})$ (Carbone and Bragg, 2020; Johnson, 2020; see these papers for a more complete spectral analysis). Thus, from this perspective, the inertial range cascade is mostly local in k (*i.e.,* nearly k_1 and k_2 are involved in the eneregy exchange), and it has significant contributions from both vortex stretching and strain self-amplification processes, but the latter effect is larger.

However, a caution is that ζ determines $\mathbf{u}$ from the Biot-Savart law, which can be written symbolically as

$$\mathbf{u} \;=\; -\,\nabla^{-2}\,[\,\nabla\times\zeta\,]\,,$$

apart from an irrotational velocity component that is trivial in a triply periodic domain, and $\mathbf{u}$ determines S. So there is nothing inconsistent with saying that the coherent vortices generated by vortex stretching control the turbulent energy cascade, even though Π_S is larger than Π_ζ.

Notice that this section again tells a story of the relative roles of strain rate and vorticity, as in Sec. 3 of the Turbulent Flows notes for the contour stretching cascade by a purely horizontal flow, where ζ and S have competing effects. Here, however, in 3D homogeneous flow they have complementary and cooperative effects in the energy.

4 Size of a Turbulent Event

How large is the dynamical system just described? The total number of degrees of freedom in turbulence, per large-eddy event, can be estimated as the volume in its space-time phase space with a discretization at the dissipation scales. The Kolmogorov scaling theory is used to answer this question. From (8),

$$\begin{aligned}\frac{L_o}{L_d} &= L_o\varepsilon^{1/4}\nu^{-3/4} \\ &= \left[\frac{\varepsilon}{V_o^3/L_o}\right]^{1/4} Re^{3/4} \end{aligned} \tag{26}$$

and

$$\frac{\tau_o}{\tau_d} \;=\; \frac{L_o}{V_o}\,\left[\frac{\varepsilon}{\nu}\right]^{1/2} \;=\; \left[\frac{\varepsilon}{V_o^3/L_o}\right]^{1/2} Re^{1/2}\,. \tag{27}$$

Thus, the total size is

$$\left(\frac{L_o}{L_d}\right)^3 \times \frac{\tau_o}{\tau_d} \;=\; \left[\frac{\varepsilon}{V_o^3/L_o}\right]^{5/4} Re^{11/4}\,. \tag{28}$$

We can interpret this as an asymptotic estimate as $Re\to\infty$ with the outer conditions held fixed (*i.e.,* the first right-hand-side term fixed). Continuity of cascade over the inertial range implies that the bracketed factors here are $\mathcal{O}(1)$ numbers.

If we make a numerical computation of this system with the usual computational stability constraint, $\Delta t < \Delta x/V_o$, then the size estimate increases slightly to $\sim\ \mathcal{O}(Re^3)$, assuming that $\Delta x < L_d$. On the face of it, this is quite daunting as a predication, based on the rate of progress in computing power (*i.e.,* a doubling of speed every ≈ 1.5 years, a.k.a. Moore's Law), for the rate of scientific progress that can be made towards this asymptotic limit. If the latter doubles every 1.5 years, the Re can be doubled every $1.5^3 \approx 3.4$ years. Thus, a direct computational assault on the turbulence problem will require great patience. However, most researchers in the field are

more optimistic than this seems to suggest: one can hypothesize that asymptotic behavior usually occurs at rather modest values of Re beyond the transition regimes around $Re \sim 10^3$, and there exist tricks of modeling the effects of unresolved scales of inertial-range motion, called *Large-Eddy Simulation* (LES), that often seem to mimic large-Re behaviors. Nevertheless, we cannot be certain about the truth of this optimism beyond the Re values accessible to direct computations, and thus we must view it as merely provisional and subject to constant testing.

Analogous to the size estimate (28), we can also use (8) to estimate the range of velocity amplitudes in turbulence,

$$\frac{V_d}{V_o} \;=\; \left[\frac{\varepsilon}{V_o^3/L_o}\right]^{1/4} Re^{-1/4}\;. \tag{29}$$

This says that small-scale fluctuations weaken only slowly with increasing Re.

5 Material Transport

Now consider material transport in 3D homogeneous turbulence. A common way to measure this is in terms of an ensemble of trajectories, $\{\mathbf{x}_\alpha(t)\}$, with a mean position $<\mathbf{x}>(t)$ and a *dispersion*,

$$D(t) \;=\; \frac{1}{2} < (\mathbf{x}(t) - <\mathbf{x}>(t))^2 > \;. \tag{30}$$

The dispersion measures the spreading of clusters of parcels, at a rate $\kappa(t) \;=\; dD/dt > 0$, and implicitly this is a mixing of neighboring parcels since there is spreading from all points. If the parcels are labeled by a property concentration c, then dispersion will effect a property flux $\overline{c'\mathbf{u}'}$ whenever there is a mean property gradient $\nabla\overline{c} \neq 0$ (see above). This is often viewed as a mixing process (Figs. 6-7).

To accompany the velocity phenomenology in the preceding section, we can hypothesize that there is also an inertial range in the scalar concentration where the fluctuation amplitude C_L on scale L depends only on the scalar cascade and dissipation rate χ and the local eddy turnover time, $\tau_L = L/V_L \sim \varepsilon^{-1/3}L^{2/3}$; *i.e.,* C_L and its associated wavenumber spectrum $E_c(k)$ are

$$C_L \sim (\chi\tau_L)^{1/2} \qquad \Rightarrow \qquad E_c(k) \sim C_L^2 L \sim \chi\tau_L L \sim \chi\varepsilon^{-1/3}k^{-5/3}\,; \tag{31}$$

i.e., it has the same wavenumber shape as the energy spectrum $E(k)$ in (17). This result is referred to as the Obukhov-Corrsin theory (see Shraiman and Siggia, 2000), and it has a non-dimensional constant factor, referred to as C_θ with an experimental value of about 0.4 (Sreenivasan, 1996), which is analogous to C_k in (17).

We can write

$$\mathbf{x}(t) \;=\; \int_0^t \mathbf{u}(\mathbf{x}(t'),t')\,dt' \tag{32}$$

in a Lagrangian reference frame and further partition both $\mathbf{x}$ and $\mathbf{u}$ into mean (*i.e.,* $<\cdot>$) and fluctuating components (*i.e.,* $\cdot'$); from (30) we see that D only depends on the fluctuating components,

$$D(t) \;=\; \frac{1}{2}\int_0^t dt' \int_0^t dt'' \;<\mathbf{u}'(t')\cdot\mathbf{u}'(t'')>\;. \tag{33}$$

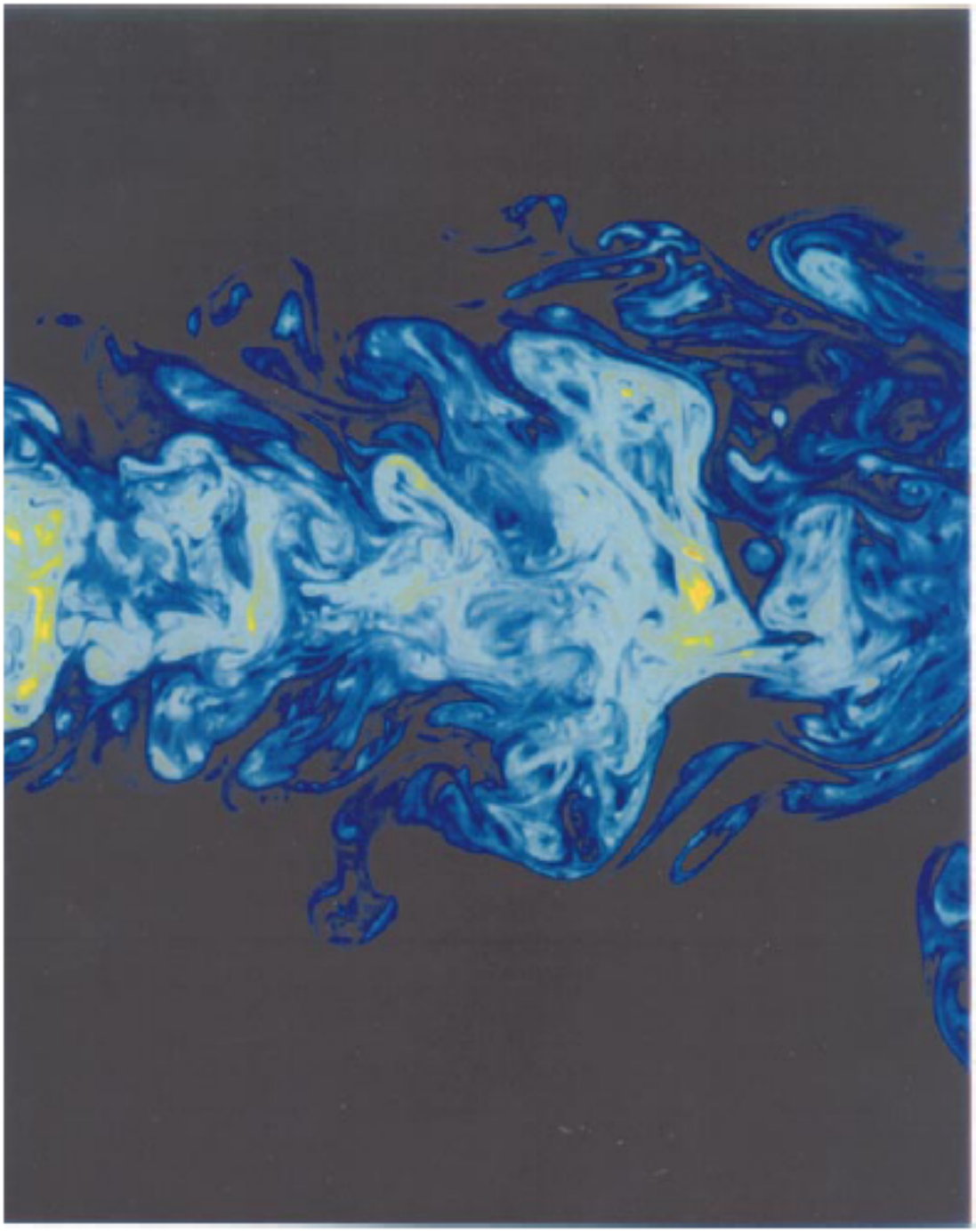

Figure 6: Fluorescent dye in a 3D turbulent jet (Shraiman and Siggia, 2000). The Re value is about 4000.

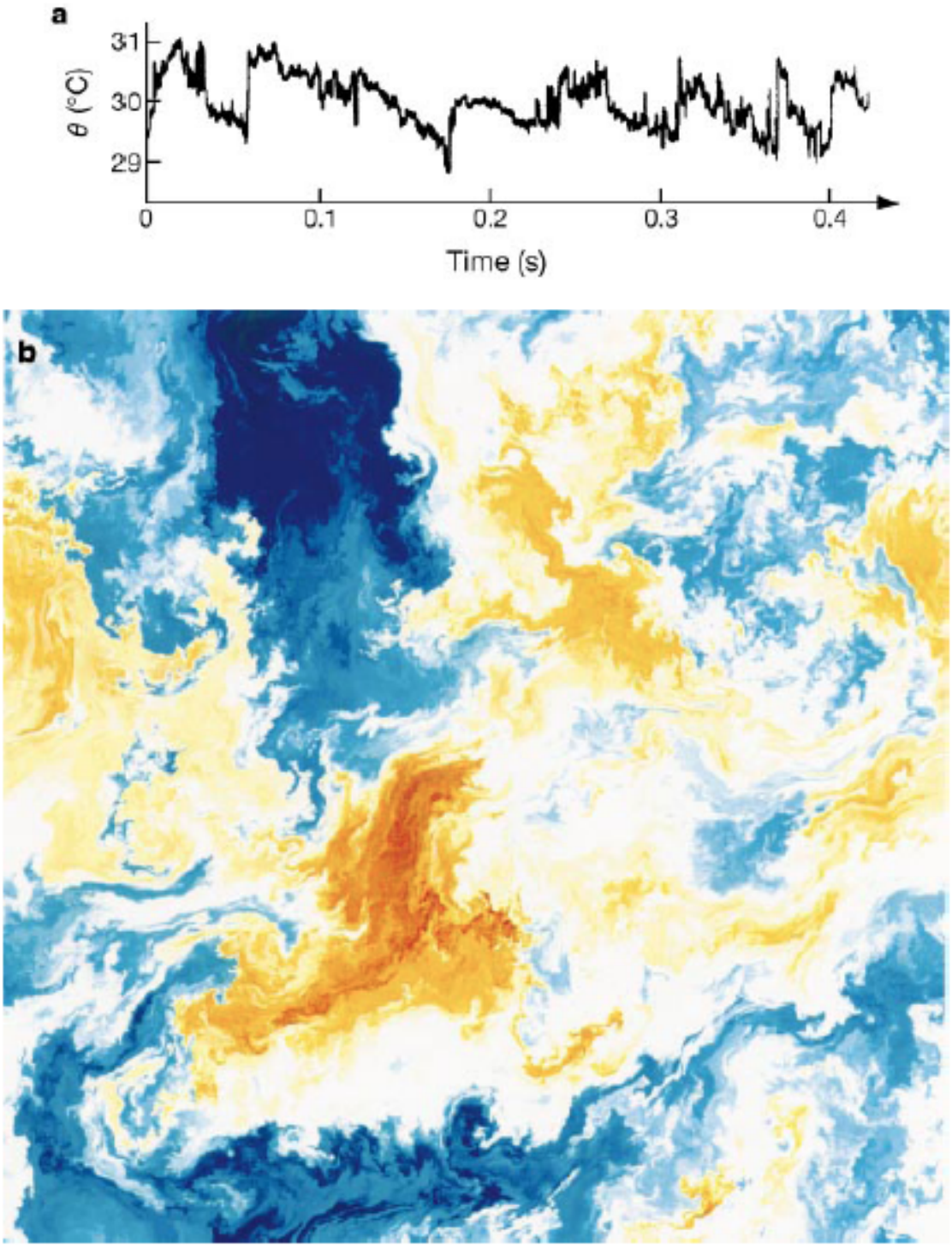

Figure 7: Scalar fluctuations in time and space. (a) Temporal trace of the temperature recorded at a fixed point in a turbulent boundary layer over a heated plate. Note the asymmetry of the derivative. (b) Numerical simulation of passive scalar advection in two dimensions for the Kraichnan (1994) model. The concentration scale runs from red to blue. (Shraiman and Siggia, 2000).

In stationary turbulence, the *Lagrangian time-lag covariance function* depends only on the magnitude of the time difference $s = |t' - t''|$ (also called time lag):

$$< \mathbf{u}'(t') \cdot \mathbf{u}'(t'') > = \sigma^2 \mathcal{C}(s), \quad \sigma^2 = < \mathbf{u}'(0)^2 > , \tag{34}$$

and the expectation based on sensitive dependence and limited predictability is that $\mathcal{C} \to 0$ as $|s| \to \infty$, *i.e.,* after an interval on the order of a large eddy (outer scale) turnover time, $\tau_o = L_o/V_o$. Thus,

$$\begin{aligned} D &= \frac{1}{2}\sigma^2 \int_0^t dt' \int_0^t dt'' \, \mathcal{C}(|t' - t''|) \\ &= \sigma^2 \int_0^t dp \int_0^p ds \, \mathcal{C}(s) \\ &\to \sigma^2 \tau_I t \quad \text{as } t \to \infty \, . \end{aligned} \tag{35}$$

For the second step we made a transformation of the time integration variables from t' and t'' to $s = t' - t''$ and $p = t' + t''$ and used the symmetry of $\mathcal{C}$ with respect to the sign of $s = t' - t''$. In the third step for the large-time asymptotic limit,

$$\tau_I = \int_0^\infty ds \, \mathcal{C}(s)$$

is the *integral time scale*, which is well defined since $\mathcal{C}$ vanishes for large s. Thus, D increases linearly at late time, just as in a random walk, and

$$\kappa = \frac{dD}{dt} \to \sigma^2 \tau_I \tag{36}$$

is the *Taylor diffusivity*. An alternative expression for κ is obtained by differentiating (33),

$$\kappa(t) = \int_0^t dt' \, < \mathbf{u}'(t - t') \cdot \mathbf{u}'(t) > \, . \tag{37}$$

From this perspective, turbulent transport looks very much like a diffusion process, where material parcels are moved between successive large eddies as if randomly. This perspective is made explicit in a stochastic model of particle position, $\mathbf{X}(t)$, *viz.,*

$$d\mathbf{x} = \mathbf{u} \, dt \, , \qquad d\mathbf{u} = -\frac{\mathbf{u} \, dt}{\tau_I} + \sigma \left(\frac{2 \, dt}{\tau_I} \right)^{1/2} d\mathbf{W} \, , \tag{38}$$

where $d\mathbf{W}$ is a Weiner process: a random increment with a Gaussian distribution and unit variance. The velocity thus has two contributions, the random perturbation plus a term which represents the memory of the previous velocity and is inversely proportional to the integral time. This term causes the velocity autocorrelations to decay in a time interval δt as an exponential $\propto \exp[-\delta t/\tau_I]$. This simple model correctly captures the early-time behavior of straight-line (a.k.a. ballistic) motion while the velocity has not yet changed, as well as the late-time behavior in (35); however, it does not accurately represent the intermediate-time behavior due to turbulent fluctuations within the inertial range (see next paragraph). This type of model is often used in estimating material dispersion

even in complex mean flows, where $\langle\, \mathbf{u} \,\rangle$ is added to the "advection" in the first equation in (38) (*e.g.,* Sawford, 2001).

Note that κ has dimensional estimates of

$$\kappa \;=\; V^2\tau \;=\; VL \tag{39}$$

for $\tau = L/V$, an eddy turn-over time. This is the basis for *mixing-length theory* (see Appendix A in *Shear Turbulence*) that says that turbulent transport is like an enhanced molecular diffusion, with diffusivity based on a characteristic turbulent velocity V and correlation time τ or length L. If we make such an estimate for the inertial range (12), then

$$\kappa_L \;=\; V_L L \;=\; V_L^2 \tau_L \;=\; \varepsilon^{1/3} L^{4/3}\,, \tag{40}$$

which is called *Richardson's Law* (apocryphally determined by throwing parsnips off a pier). It says that a small patch of material with scale L will spread at an accelerating rate as L grows, up to a limiting scale L_o, where the diffusivity approaches the constant Taylor form (36), assuming $\tau_I \sim \tau_o$. We can alternatively view the patch spreading as a function of time,

$$\begin{aligned} D_L \quad &\sim V_L^2 \tau_L^2 = L^2 = \varepsilon \tau_L^3 \\ \kappa_L \quad &\sim V_L L = \varepsilon^{1/3} L^{4/3} = \varepsilon \tau_L^2\,. \end{aligned} \tag{41}$$

Both in size and elapsed time, the material spreading goes faster as the patch gets bigger, up to the limiting scale L_o.

For a modern review of turbulent mixing, see Srinivasan (2018).

6 Predictability

Turbulent flows have sensitive dependence and limited predictability horizons. If a LES calculation or measurements are made with a smallest resolved scale $L_* = 1/k_*$, then there necessarily is ignorance of any information on all smaller scales. With time the influence of this ignorance will spread to larger scales, including the ones being calculated or measured, contaminating their *predictability*. Metais and Lesieur (1986) suggested the following phenomenological relation to describe the spreading of the predictability horizon, expressed as the smallest uncontaminated scale $L_p = 1/k_p$:

$$\frac{dk_p}{dt} \;=\; -\frac{k_p}{\tau_k}\,, \tag{42}$$

where $1/\tau_k \;=\; \varepsilon^{1/3} k^{2/3}$ from (12) as long as k_p lies within the inertial range. Here we must solve the equation

$$\frac{dk_p}{dt} \;=\; -\varepsilon^{1/3} k_p^{5/3}\,. \tag{43}$$

The solution is

$$k_p^{-2/3} - k_*^{-2/3} \;=\; c\varepsilon^{1/3} t\,. \tag{44}$$

Assuming $k_*^{-2/3}$ is small enough, and evaluating this at the finite predictability time T_p when the contamination has spread throughout the spectrum to the outer wavenumber $k_p = 1/L_o$,

$$L_o^{2/3} \;=\; c\varepsilon^{1/3} T_p\,. \tag{45}$$

Since $\varepsilon \sim V_o^3/L_o$, this indicates that $T_p \sim L_o/V_o$; *i.e.,* all predictability is lost within a few large eddy turn-over times.

This argument implicitly assumes *scale locality* for the important dynamics within the inertial range, as do most of the scaling relations as a function of L in Secs. 2-5: nonlinear advective effects at a scale L are dominated by interactions with adjacent scales only slightly larger and smaller. As we will see in *2D Homogeneous Turbulence*, this is not true for turbulent systems with a steeper $E(k)$, where the outer scale flow, V_o at L_o, can also be influential for all smaller L.

7 Intermittency

Turbulent flows are intermittent. Intermittency means that distinctive events are rare in some sense. This is the opposite to their occurring nearly all the time. It also can be viewed as the opposite to self-similar, defined as statistically equivalent on all scales and at all locations. Thus, Brownian motion is self-similar (Fig. 8), and it is very different from a time series of velocity in turbulence (Fig. 9) that shows bursts of high-frequency fluctuations separated by quieter intervals. There is, as yet, no complete understanding of the nature of turbulent intermittency, although it is fundamentally related to the coherent structures that occur (Sec. 8). A particular statistical measure of turbulent flows is the "single-point" distribution function of any measurable variable. One example, for acceleration, was given in *Turbulent Flows: General Properties*. Another example is shown in Fig. 10 from $\sim$ 3D homogeneous turbulence, for both a passive scalar (weak temperature variations) and a velocity difference, δV_L over a separation length L within the inertial range. Note that both distributions have approximately the shape of an exponential function, with a probability of occurrence $P(a)$ of a single-point value a like

$$P(a) \ \propto \ e^{-c|a|/\sqrt{\langle a^2 \rangle}} \, , \tag{46}$$

at least in the tails of the distribution away from $a = 0$. This distribution can be called intermittent, in the sense that it has much stronger tails than any Gaussian distribution, with $P \ \propto \ e^{-c|a|^2}$. It also seems to be almost universally found in turbulent flows, in all regimes, albeit with some variety in the c values and even in the power of a in the exponent (a.k.a. a *stretched exponential* distribution), but no satisfactory "universal" explanation has been found yet.

A different statistical measure of intermittency comes from the family of *velocity-moment structure functions* for velocity differences and their functional dependence on spatial separation distances L within the inertial range:

$$< |\delta V_L|^n > \sim \ V_o^n \left[\frac{L}{L_o} \right]^{\zeta_n} \tag{47}$$

for positive integer values of n. The focus is on the family of exponents $\{\zeta_n\}$, that can be measured experimentally (albeit with an statistical sampling uncertainty rapidly increasing with n) and fit with various statistical models (*e.g.,* Fig. 11). The Kolmogorov (1941) cascade theory, which is implicitly not intermittent by hypotheses H2-H3, implies $\zeta_n = n/3$, which is clearly not confirmed. A generalization — the β-model of Frisch *et al.* (1978) that assumes that only a progressively smaller fraction of the fluid volume is active as the cascade progresses towards small scales — implies $\zeta_n = 1 + (n-3)h$ and thus relates the intermittency exponents to a scaling-symmetry

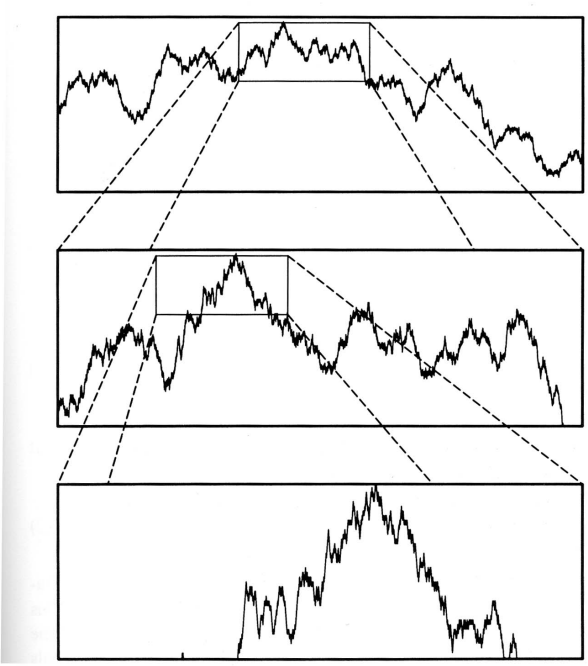

Figure 8: Brownian motion: a portion of a time series $y(t)$ for a random velocity increment $v(t)dt$, enlarged twice, illustrating its self-similarity (*i.e.,* scale invariance). (Frisch, 1995)

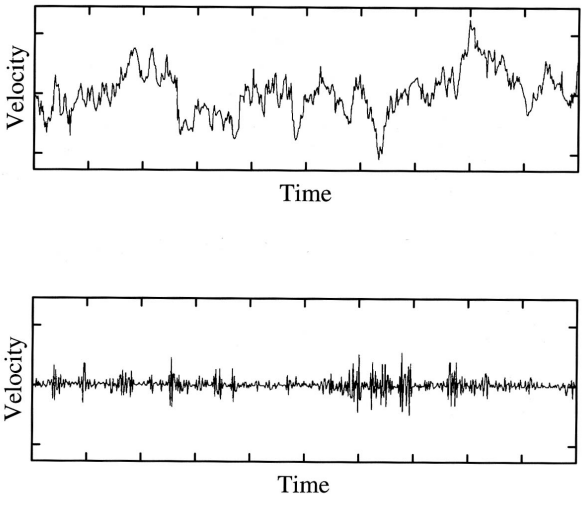

Figure 9: (Top) Velocity signal from a jet with $Re_\lambda \approx 700$. (Bottom) Same signal as in (a) subject to high-pass filtering showing intermittent bursts. (Gagne, 1980)

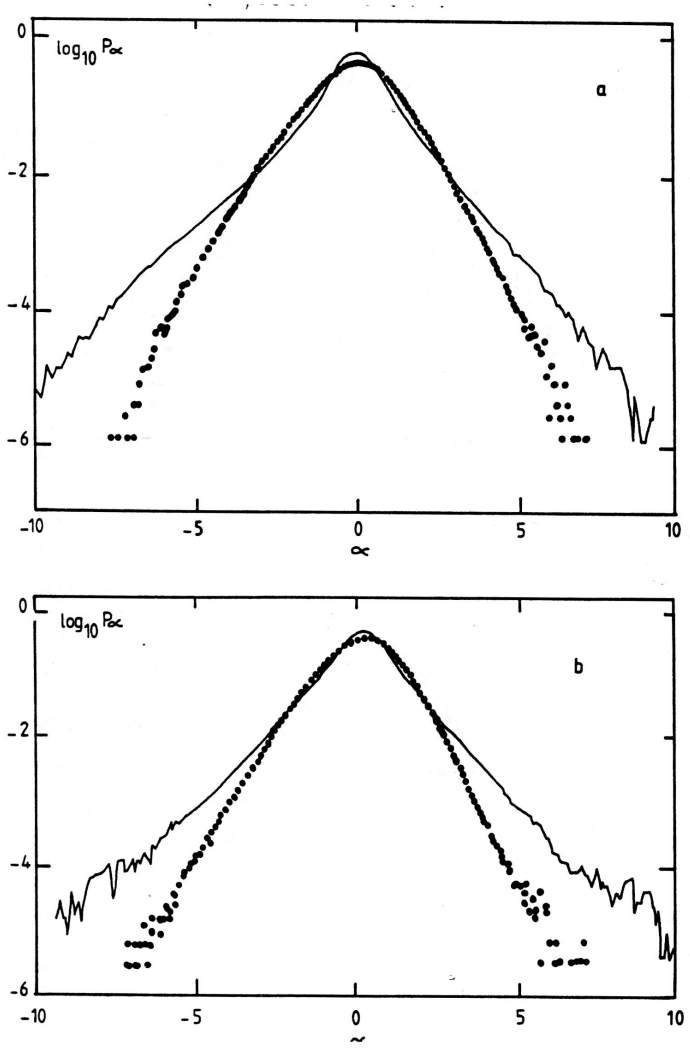

Figure 10: Single-point, single-quantity PDFs $p[\alpha]$ for temperature (continuous line) and velocity increment (between separated points), where α is the quantity normalized by its standard deviation. The panels are for different increment separation distances: (a) jet, with distance $r/\eta = 100$; (b) wind tunnel, with distance $r/\eta = 1307$. (Castaing *et al.*, 1990)

exponent h different from the $h = 1/3$ value in (13); however, it too is not well supported by data. A model based on a log-normal distribution is not as bad a fit as these others models. She and Leveque (1994) devised a *hierarchical structure model* using the so-called *log Poisson* distribution that implies $\zeta_n = n/9 + 2[1 - (2/3)^{n/3}]$; based on the data in Fig. 11 and subsequent experiments, this latter model seems to fit the data quite well. Nevertheless, the estimation uncertainty is large for $\{\zeta_n\}$, and a statistical fit is certainly not a dynamical theory for the intermittency of turbulence. More recently, Lundgren (2008) proposed an alternative statistical model that is at least as successful in fitting empirical intermittency measures. It implies that the spatial "dimension" d of the near-singularities in the flow that contribute most to dissipation rate ε is $d \approx 2.8$, indicating that the cascade of 3D turbulence is nearly, but not quite, volume-filling. Finally, Benzi *et al.*(1993) *et seq.* have established the experimental validity of *Extended Self-Similarity* (ESS) with the same exponent set, $\{\zeta_n\}$, for all values of Re, thus demonstrating that the nature of the intermittency in turbulence is the same even outside the idealized $Re \to \infty$ limit where a well-defined inertial range occurs (but still for L values much larger than η); of course, the degree of intermittency does increase with Re.

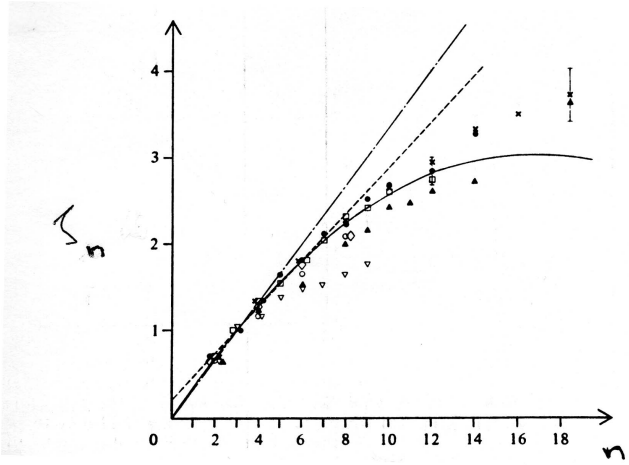

Figure 11: Variation of exponent ζ_n as a function of the order n from different experiments with different Re values. The curves are various model fits: the dash-dot line is from Kolmogorov (1941); the dashed line is the β model of Frisch *et al.* (1978), and the solid line is from a log-normal distribution. (Anselmet *et al.*, 1984)

The fact of increasing intermittency with Re is shown with some rather more direct measures in Fig. 12: the experimentally measured skewness Sk and kurtosis (or flatness) Ku (or F) (*i.e.,* the averaged third and fourth powers of a single-point quantity suitably normalized by the variance raised to the powers 1.5 and 2, respectively) for a longitudinal velocity derivative and a passive scalar derivative as functions of Re. For a quantity with a Gaussian probability distribution function, the skewness is zero and the kurtosis is 3.0[3]. Large values of the statistical measures indicate probability distributions with high probability of large values, *i.e.,* intermittency. As we see, all of these measures are increasing functions of Re up to as high as has been measured; their dependen-

[3]Be careful about definitions. Often F is used as synonymous with Ku (as here). Sometimes, though, $F = Ku/3 - 1$ is used, so that F becomes a normalized measure of the non-Gaussianity.

cies have approximately a power-law form, with

$$Sk(\partial u/\partial x) \sim Re^{1/8}, \;\; F(\partial u/\partial x) \sim Re^{1/3}, \;\; F(\partial\theta/\partial x) \sim Re^{1/2} \, . \tag{48}$$

This shows that turbulence has a degree of intermittency that increases without bound as the Re increases. Thus, if there is a hope of understanding the behavior in nature at larger values of Re than can be achieved in computations or controlled experiments, it is to be able to identify suitable scaling relations, like those above, and extrapolate them in Re to the naturally occurring regimes. These scaling exponents for Sk and F are consistent with the statistical model of Lundgren (2008).

The intermittency of a passively advected-diffused scalar $c(\mathbf{x}, t)$ is accessible to a more complete and rigorous mathematical analysis than velocity $\mathbf{u}(\mathbf{x}, t)$ when the former problem is posed under the simplifying assumption that the advecting velocity field is a Gaussian random variable satisfying the incompressibility constraint (*i.e.,* not a $\mathbf{u}(\mathbf{x}, t)$ from a real turbulent flow; see the review article by Shraiman and Siggia, 2000).

8 Vortex Stretching and Coherent Vortices

Vortex stretching was introduced in *Turbulent Flows: General Properties* as a mechanistic explanation of the energy cascade. Here we revisit the process as a basis for understanding the widespread occurrence of *vortex tubes* in 3D homogeneous turbulence as a particular manifestation of *coherent structures* in different turbulent regimes.

We form the vorticity equation by taking the curl of the momentum equation in (1). Using index notation, it can be written as

$$\frac{D\zeta_i}{Dt} \;=\; \zeta_j S_{ij} + \nu\nabla^2\zeta_i \, , \tag{49}$$

where S_{ij} is the *strain-rate* or *deformation-rate tensor*, *i.e.,* the symmetric part of the velocity-gradient tensor,

$$S_{ij} \;=\; \frac{1}{2}\left(\frac{\partial u_i}{\partial x_j} + \frac{\partial u_j}{\partial x_i}\right) \, . \tag{50}$$

The interesting term here is the first one on the right-hand side of (49); it describes the stretching and turning of vortex lines (Fig. 13).

The turbulent cascade of 3D turbulence is often associated with vortex stretching, whereby a vortex tube is turned to become aligned with the axis of strain and then becomes longer through stretching that causes its radius to shrink and its vorticity amplitude to grow (while preserving its circulation, $\int\int \zeta \, dA$, as Kelvin's theorem requires). In the inertial range, an estimate for the vorticity amplitude ζ_L is

$$\zeta_L \;=\; \frac{V_L}{L} \;=\; \frac{(\varepsilon L)^{1/3}}{L} \;=\; \varepsilon^{1/3} L^{-2/3} \, , \tag{51}$$

which increases as L decreases. The dominant energy is thus at the outer scale, while the dominant vorticity (*i.e.,* enstrophy) is at the Taylor microscale or even the smaller Kolmogorov dissipation scale.

We can illustrate this process with a simple solution that generalizes the solution in *Turbulent Flows: General Properties*. Consider the case of a purely straining background flow that is

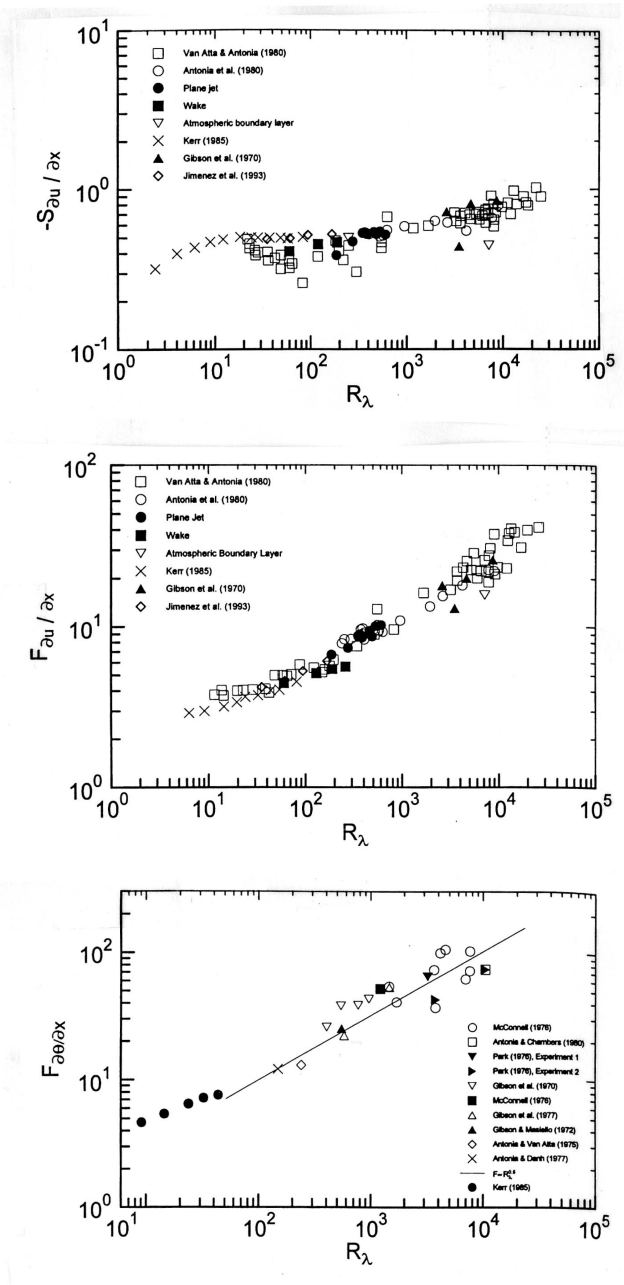

Figure 12: Variations of skewness and kurtosis with Re_λ in 3D homogeneous turbulence from various experiments: (top) $-Sk(\partial_x u)$; (middle) $Ku((\partial_x u)$; (bottom) $Ku((\partial_x T)$. (Sreenivasan and Antonia, 1997)

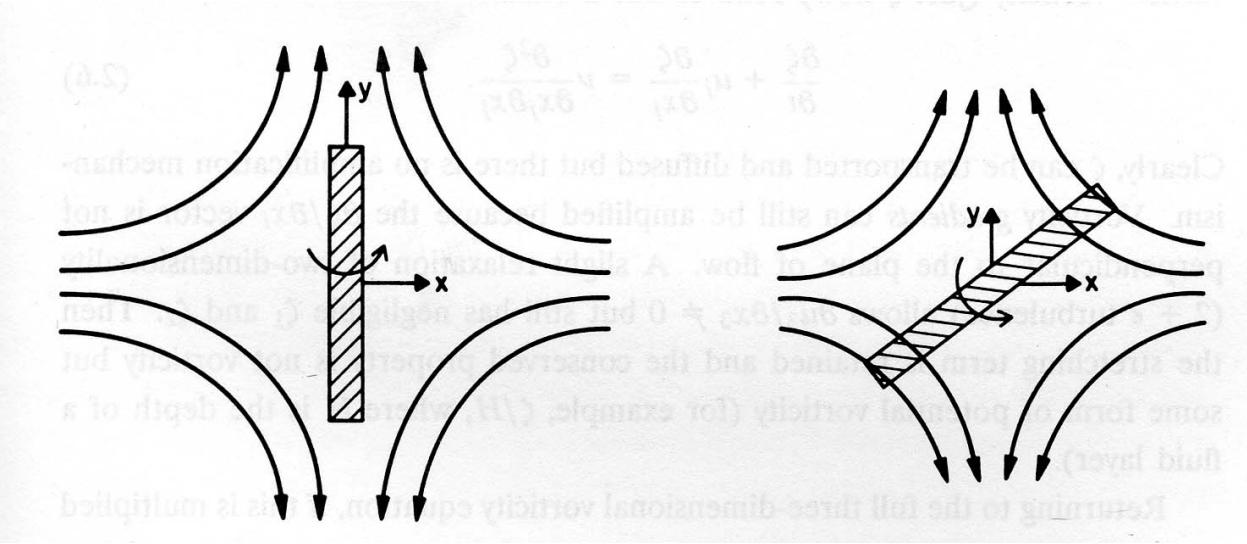

Figure 13: (Left) The increase of ζ_y by stretching ($\zeta_x = \zeta_z = 0$). (Right) The change of ζ_y by turning the vorticity vector. (Tennekes, 1989)

axisymmetric about the $\hat{\mathbf{z}}$ axis. In cylindrical coordinates,

$$\mathbf{U} \;=\; (-sr,\; 0,\; 2sz)\;. \tag{52}$$

The equation for the vertical component of vorticity ζ^z for deviations from the background flow is therefore

$$\frac{D\zeta^z}{Dt} \;=\; 2s\zeta^z + \nu\nabla^2\zeta^z\;. \tag{53}$$

This has a self-similar solution for vorticity and azimuthal velocity of the form

$$\begin{aligned} \zeta^z(r,t) &= \frac{\Gamma}{4\delta^2}e^{-r^2/4\delta^2} \\ u^\phi(r,t) &= \frac{\Gamma}{2\pi r}\left[1 - e^{-r^2/4\delta^2}\right]\;, \end{aligned} \tag{54}$$

where the vortex tube radius δ is

$$\delta^2 \;=\; \frac{\nu}{s} + \left[\delta_o^2 - \frac{\nu}{s}\right]e^{-st}\;. \tag{55}$$

This describes an exponentially stretching, narrowing, intensifying vortex that ultimately reaches a steady-state balance between stretching and viscous diffusion on a scale $L_v \;=\; (\nu/s)^{1/2}$ that is equivalent to the Taylor microscale, λ in (18), for this situation. This final state solution is called Burger's vortex.

The viscously-arrested vortex tube is a paradigm for the coherent structures of 3D homogeneous turbulence, vortex tubes or vorticity filaments (or even "worms"). By computational and experimental techniques, tubes have been shown to be ubiquitously present in this turbulent regime (Figs. 14-16), albeit not exactly in the stationary state of (55) but with associated movement, deformation, creation, and destruction phases of their life cycles.

Coherent structures were discussed in *Turbulent Flows: General Properties*, particularly in reference to the competition between vorticity and strain in non-divergent horizontal flows where the vorticity-dominated regions of the flow have a more persistent, hence coherent, evolution. We will encounter coherent structures in each of the physical regimes of geophysical turbulence. Their particular shape and dynamics vary with the regime, but they also have many attributes in common across regimes. The following is a working definition of a coherent structure that is not overly tied to any particular regime:

- a recurrent, spatially local *pattern* in the fields, especially in $\zeta = \nabla \times \mathbf{u}$.
- a *preferred state* with respect to the conservative nonlinear fluid dynamics, permitting self-organization of the flow by dissipative evolution towards an attractor.
- *spatially isolated* from each other, hence dynamically weakly coupled, most of the time; thus, intermittent in their strong coupling events (*e.g.,* where dissipation occurs most strongly).
- *long-lived* in a Lagrangian reference frame; thus, weakly dissipative over most of its lifetime and capable of "anomalous" material transport (*i.e.,* different from $D \propto t$ or the appropriate inertial-range power-law, *e.g.,* t^3 in (41) for 3D homogeneous turbulence).

Many scientists, including me, believe that the investigation of coherent structures is one of the most fruitful paths in turbulence research. A formalization of this opinion is the *hypothesis of ubiquity and dynamical control*:

> Turbulent motions at large Re develop coherent structures whose dynamics govern the aggregate properties of the flow, such as the transport and dissipation, in combination with other influences from the macroscopic forcing and damping (hence mean circulations), wave propagation, and boundaries.

This hypothesis has yet to be fully proved, although it is perhaps close to being well demonstrated in *2D Homogeneous Turbulence*. It can be rather subtle to devise ways to test and/or demonstrate the hypothesis.

The coherent structures of 3D homogeneous turbulence, vortex tubes, do conform to this definition, although less strongly so in several ways than the structures of other regimes. Their pattern is one of strong vorticity amplitude aligned along a long axis with length $\sim L_o$ and a much narrower width $\sim \lambda$. The latter means that they are of relatively small scale, compared to less isotropic regimes where the coherent structures often occur over a wider range of sizes. Their associated velocity field is an azimuthal swirl about the vorticity axis; thus, locally the flow is anisotropic, approximately axisymmetric, and "horizontally" non-divergent. However, the orientation of this axis is arbitrary, and isotropy is recovered after averaging over many coherent vortices. The dynamically preferred or selected state of vortex tubes is represented by the self-similar solution (54) for vortex stretching in a large-scale strain field: given a more complex initial condition for the fluctuation field, this is the one that comes to dominate with time, while the other components are more vulnerable to cascading to dissipation, particularly once the vortex flow adds to their ambient strain field. The vortex tubes are usually isolated from each other (Figs. 14-16), but when the large-scale flow pushes them together, they can undergo a *vortex reconnection* event (Fig. 17) that

involves substantial dissipation; usually the reconnections are local switches in the connectivity of the approaching vortex lines, but in extreme cases of globally parallel and anti-parallel approaches, the outcomes are combined by merger and or annihilation, respectively. Vortex reconnection is an extreme event in its scale contraction and vorticity amplification; it has even been shown to be a plausible candidate for a finite-time singularity of the Euler equations (*i.e.,* with $\nu = 0$); see Kerr (1993), but see also a skeptic's statement by Frisch (1995), and a general discussion of the mathematical structure of a possible instability in Majda and Bertozzi (2002). My own view is that this issue is unsettled for lack of a sufficiently clean computational test, though it remains a hot topic in the literature. Vortex lifetimes are on the order of a large-eddy turnover time τ_o except when close encounters occur sooner. The rationale for this is that the tubes are sustained by being correctly aligned with the large-scale strain field, and when the latter changes faster than the vortex can follow by turning, then the tube configuration loses stability, through *vortex breakdown*. This lifetime is rather short compared to more anisotropic flow regimes, where the coherent structures often persist for many τ_o. The potential for anomalous transport is due to the tendency of parcels near a tube to stay near it, since the flow is primarily recirculating. The hypothesis that vortex tubes control the Kolmogorov cascade in 3D homogeneous turbulence has not yet been substantially proved, although Chorin (1994) presents arguments in this direction. On the other hand, it seems quite plausible that the intermittency statistics of this regime are the consequence of the structure and dynamics of tubes, although this too has not been convincingly shown (but see the discussion in Frisch, 1995).

Readings

1. Stewart and Garrett (2004) [an enticement article for high school mathematics students; `http://media.pims.math.ca/pi_in_sky/pi8.pdf`.]

2. Sreenivasan (1990) [a News and Views article in *Nature*] **344**, 192-193, entitled "Turbulence and the tube".]

References

Anselmet, F., Y. Gagne, E.J. Hopfinger, and R.A. Antonia, 1984: High-order velocity structure functions in turbulent shear flow. *J. Fluid Mech.* **140**, 63-89.

Benzi, R., S. Ciliberto, R. Tripiccione, C. Baudet, F. Massaioli, , and S. Succi, 1993: Extended self-similarity in turbulent flows. *Phys. Rev. E* **48**, R29-R32.

Bonn, D. Y. Couder, P.H.J. van Dam, and S. Douady, 1993: From small scales to large scales in 3D turbulence: the effect of diluted polymers. *Phys. Rev. E* **47**, R28-R31.

Carbone, M., and A.D. Bragg, 2020: Is vortex stretching the main cause of the turbulent energy cascade? *J. Fluid Mech. Rapids* **883**, R2.

Castaing, B., Y. Gagne, and E. Hopfinger, 1990: Velocity probability density functions of high Reynolds number turbulence. *Physica D* **46**, 177-200.

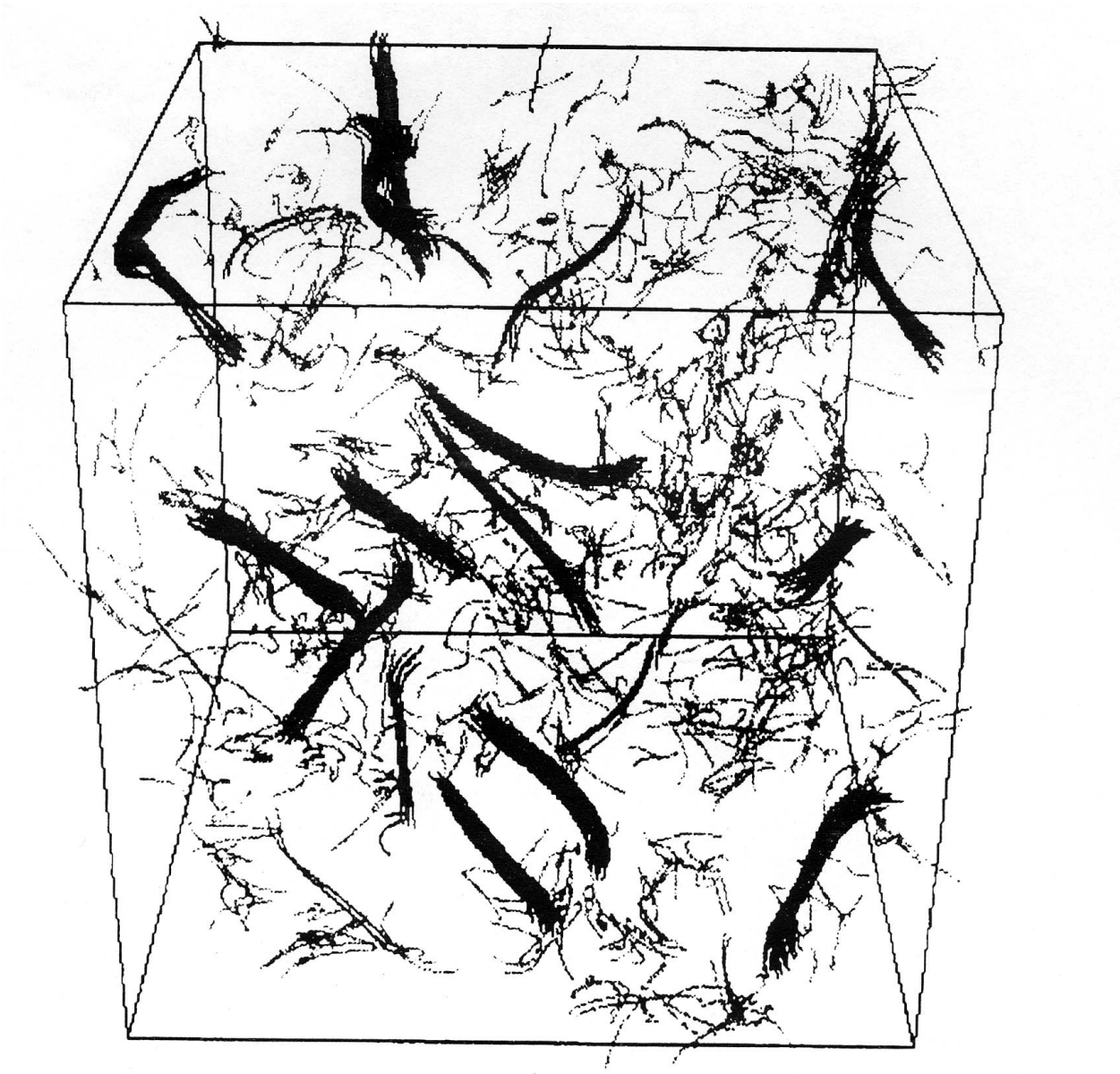

Figure 14: Intermittent vortex filaments in a 3D computational simulation of equilibrium homogeneous turbulence. (She *et al.*, 1991)

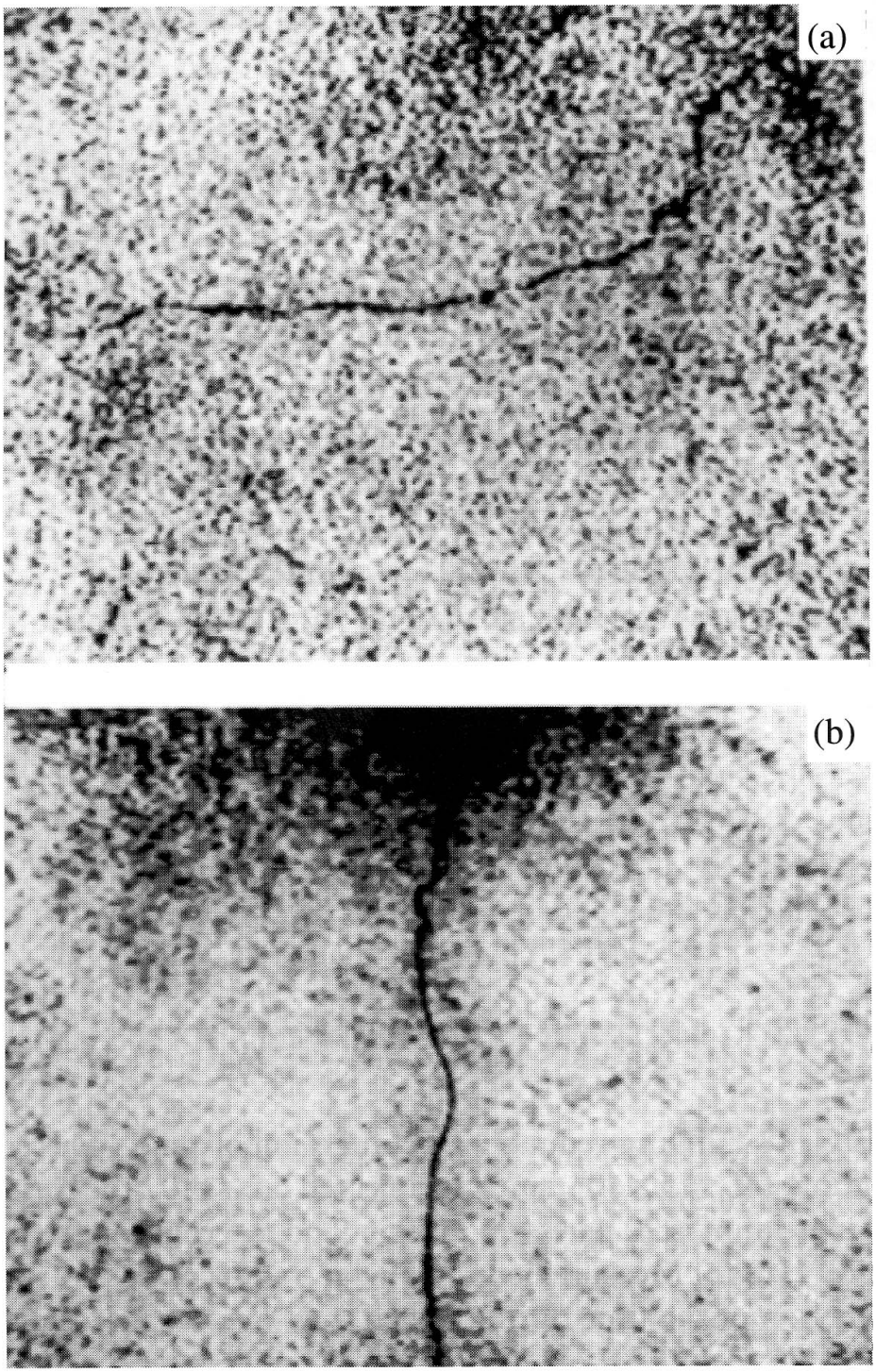

Figure 15: Two images of high concentrations of vorticity obtained in water seeded with small bubbles for visualization. The tank is lit with diffusive light from behind, and the bubbles appear dark: (a) a vorticity filament in $\sim$ homogeneous 3D turbulence; the core of an axial vortex below a rotating disk (*i.e.,* a pseudo-tornado). (Bonn *et al.*, 1993)

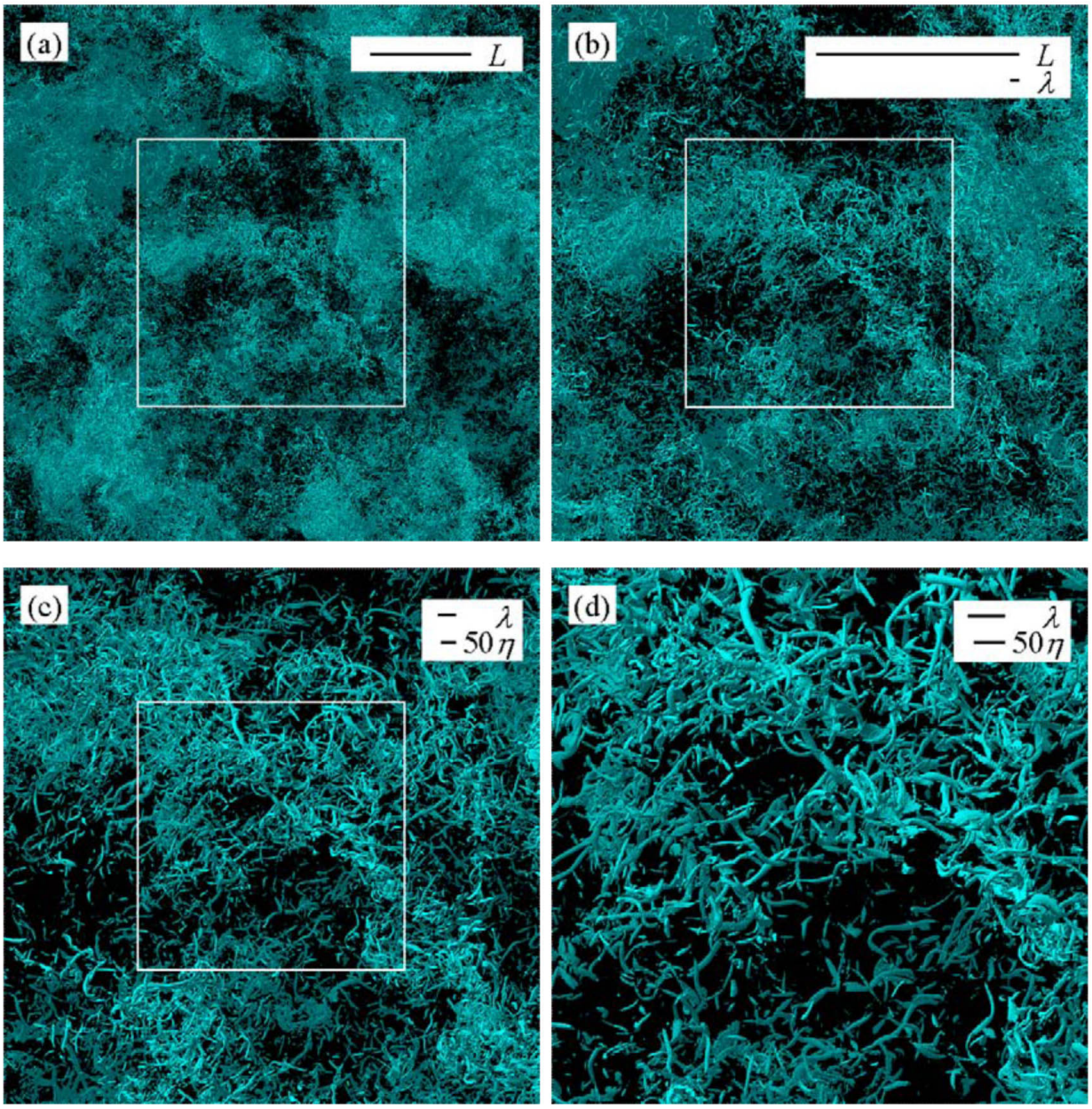

Figure 16: $|\zeta|$ iso-surfaces at several magnifications in a computational simulation of randomly forced, 3D, isotropic, homogeneous turbulence. (L, λ, η) = forcing, Taylor, and Kolmogorov scales. (Kaneda, 2005)

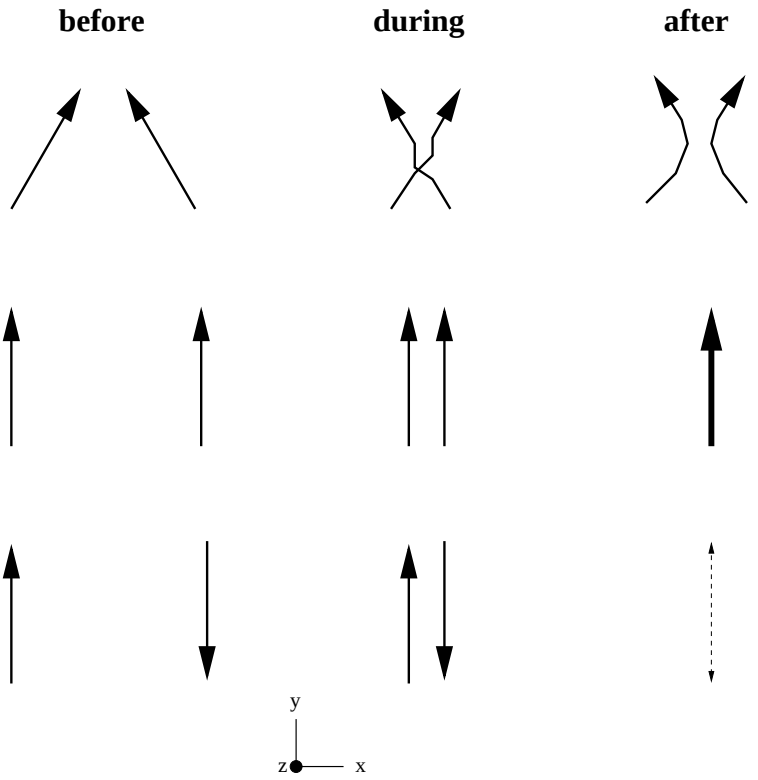

Figure 17: Vortex reconnection: the initial orientations of a pair of neighboring vortex tubes is indicated in the left column. They are advected closer together in the middle column, and their configurations after reconnection are in the right column.

Chen, S.Y., G. Doolen, J.R. Herring, and R. Kraichnan, 1993: Far-dissipation range of turbulence. *Phys. Rev. Lett.* **70**, 3051-3054.

Chorin, A.J., 1994: *Vorticity and Turbulence*. Springer.

Frisch, U., P.L. Sulem, and M. Nelkin, 1978: A simple dynamical model of intermittent, fully developed turbulence. *J. Fluid Mech.* **87**, 719-736.

Frisch, U., 1995: *Turbulence*, Cambridge.

Gagne, Y., 1980: Ph.D. Thesis, Universite de Grenoble.

Gagne, Y., and B. Castaing, 1991: A universal representation without global scaling invariance of energy spectra in developed turbulence. *C.R. Acad. Sci. Paris, II* **312**, 441-445.

Gibson, C.H., and W.H. Schwarz, 1963: The universal equilibrium spectra of turbulent velocity and scalar fields. *J. Fluid Mech.* **16**, 365-384.

Grant, H.L., R.W. Stewart, and A. Moillet, 1961: Turbulence spectra from a tidal channel. *J. Fluid Mech.* **12**, 241-263.

Johnson, P.L., 2020: Energy transfer from large to small scales in turbulence by multiscale nonlinear strain and vorticity interactions. *Phys. Rev. Lett.* **124**, 104501.

Kaneda, Y., 2005 (personal communication). See also Kaneda, Y., T. Ishihara, M. Yokokawa, K. Itakura, and A. Uno, 2003: Energy dissipation rate and energy spectrum in high resolution direct numerical simulations of turbulence in a periodic box. *Physics of Fluids* **15**, L21-L24.

Kerr, R.M., 1993: Evidence for a singularity of the three-dimensional, incompressible Euler equations. *Physics of Fluids A* **5**, 1725-1746.

Kolmogorov, A.N., 1941: The local structure of turbulence in an incompressible viscous fluid **and** On degeneration of isotropic turbulence in an an incompressible viscous fluid **and** Dissipation of energy in locally isotropic turbulence. *Dokl. Acad. Nauk. S.S.S.R.* **30**, 301-305 **and 31**, 538-541 **and 32**, 16-18.

Kraichnan, R.H., 1994: Anomalous scaling of a randomly advected passive scalar. *Phys. Rev. Lett.* **72**, 1016-1019.

Ladyzhenskaya, O., 1969: *The Mathematical Theory of Viscous Incompressible Flows*, Gordon and Breach.

Lundgren, T.S., 2008: Turbulent scaling. *Phys. Fluids* **20**, 031301 – 1-10.

Majda, A., and A. Bertozzi, 2002: *Vorticity and Incompressible Flow*, Cambridge.

Metais, O., and M. Lesieur, 1986: Statistical predictability of decaying turbulence. *J. Atmos. Sci.* **43**, 853-870.

Sawford, B.L., 2001. Turbulent relative dispersion. *Annual Review of Fluid Mechanics* **33**, 289-317.

She, Z.-S., Jackson, and S. Orsag, 1991: Structure and dynamics of homogeneous turbulence: models and simulations. *Proc. Roy. Soc. London A* **434**, 101-124.

She, Z.S., and E. Leveque, 1994: Universal scaling laws in fully developed turbulence. *Phys. Rev. Lett.* **72**, 336-339.

Shraiman, B., and E. Siggia, 2000: Scalar turbulence. *Nature* **405**, 639-646.

Sreenivasan, K., 1990: Turbulence and the tube. *Nature* **344**, 192-193.

Sreenivasan, K., 1996: The passive scalar spectrum and the Obukhov–Corrsin constant. *Phys. Fluids* **8**, 189-196.

Sreenivasan, K., and R.A. Antonia, 1997: The phenomenology of small-scale turbulence. *Ann. Rev. Fluid Mech.* **29**, 435-472.

Sreenivasan, K., 2018: Turbulent mixing: A perspective. *P.N.A.S.* **116**, 18175-18183.

Stewart, R., and H. Townsend, 1951: Similarity and self-preservation in isotropic turbulence. *Phil. Trans. Roy. Soc. London A* **243**, 359-386.

Stewart, R., and C. Garrett (2004): Kolmogorov, Turbulence, and British Columbia. π *in the Sky* (8), 22-23. [`http://www.pims.math.ca/pi/`]

Tennekes, H., 1989: Two- and three-dimensional turbulence. In: *Lecture Notes on Turbulence*, J.R. Herring and J.C. McWilliams (eds.), 1-73.